Near-Wakes of Elliptic Cylinders in Subcritical Flow

V. J. MODI* AND A. K. DIKSHIT†
University of British Columbia, Vancouver, B.C., Canada

The near-wake aerodynamics of a set of two-dimensional, stationary, elliptic cylinders is studied experimentally during the organized wake condition (Reynolds number = 68,000) as a function of the cylinder eccentricity and angle of attack, An extensive scanning of the pressure field provides useful information concerning the vortex formation region, longitudinal and lateral spacings between the vortices, the classical wake geometry ratio, and the vortex velocity. A flow visualization study through the Schlieren technique in conjunction with high-speed photography gives preliminary information about location of the separating shear layers, their oscillations, and position of the first vortex. The rise and decay of the unsteady pressure in the vortex formation region appears to substantiate the visual observation concerning the first vortex.

Nomenclature

C_{Dh} = mean drag coefficient based on the projected height, pressure drag/$\{(1/2)\rho V_\infty{}^2 2ah\}$
C_p = mean static pressure coefficient, $(p-p_\infty)/\{(1/2)\rho V_\infty{}^2\}$
$\overline{F}$ = ratio of the maximum fluctuating pressure (average amplitude) at a transverse station in the wake to the corresponding value on the surface of the model for a given angle of attack, $\overline{p'_w}/(\overline{p'_m})_{\max}$
L = longitudinal spacing between vortices
R = Reynolds number, $V_\infty 2a/\nu$
S_h = Strouhal number based on the projected height of the model, fh/V_∞
V_v = streamwise vortex velocity
V_∞ = freestream velocity
W = lateral spacing between vortices
a = semi-major axis of the model
b = semi-minor axis of the model
e = eccentricity of an elliptic cylinder, $[1-(b/a)^2]^{1/2}$
f = frequency of shedding vortices, Strouhal frequency
h = projected height of the model normal to the freestream
p = mean pressure
$\overline{p'}$ = amplitude of fluctuating pressure signals
$\overline{p'}$ = unsteady pressure (average amplitude based on the rms value) about mean
p_∞ = mean static pressure in the freestream
x, y = reference co-ordinate system with origin on the axis of a model at the central section, x in the downstream direction and y along the cylinder axis
α = angle of attack
ν = kinematic viscosity of air
ρ = air density
ϕ = phase angle between fluctuating pressure signals

Subscripts

m = parameter value on the model surface
max = maximum value of parameter
p = pitch
w = parameter value in wake
y = yaw

I. Introduction

STROUHAL was the first to correlate the periodic vortex shedding with the diameter of a circular cylinder and fluid velocity. This was followed by the classical study of von Kármán, wake analysis by Heisenberg, and experiments on wake geometry by Bénard. Ever since, academic and practical interest in the vortex shedding phenomenon have resulted in many theoretical and experimental investigations of considerable significance. Rosenhead,[1] Wille,[2,3] Marris,[4] Morkovin,[5] and Slater[6] have reviewed this literature at some length. It would be sufficient, therefore, to emphasize only the important features of the available information more directly relevant to the present investigation. Three regions can be identified in the wake of a bluff body: 1) the immediate vicinity of the body, constituted by the region approximately 1 diam downstream, where the separated shear layers undergo transition to turbulence before rolling into turbulent vortices; 2) the intermediate region of the organized Kármán vortex street; and 3) the far wake, where the vortices diffuse and dissipate forming a turbulent field. Much of the available literature is concerned with the last region.[7] In the current investigation the interest is confiend to 1) and 2), the region referred to here as "near-wake."

In the near-wake, the lengths after which transion to turbulence occur and the appearance of the first vortex (the formation length) are given as functions of the Reynolds number by Bloor and Gerrard.[8,9] The transion length has its importance in the determination of the vortex strength while the formation length is necessary for predicting the unsteady pressure intensity. Investigations related to the vorticity content of the separated shear layer, the mechanism of vortex formation and vortex strength were undertaken by Fage and Johansen,[10] Abernathy and Kronauer,[11] Gerrard,[12] Bloor and Gerrard,[8] and others. It was found that the strengths of the two separated shear layers are equal for even unsymmetrical bodies and proportional to the base pressure parameter. For a symmetrical body, there is a loss of about 35% of the available vorticity during formation of a vortex from the separating shear layer.

Several length parameters associated with the near-wake have been found important in predicting the shedding frequency. The normal distance between the separated shear layers before they roll into vortices was proposed by Roshko.[13] The others have been the formation length and transverse distance between the separation points suggested by Gerrard[12] and Dikshit,[14] respectively.

In the intermediate region the vortices are organized in a constant longitudinal spacing, L, and the increasing lateral spacing, W, as they travel downstream. The geometry of a turbulent vortex as well as its velocity field are not yet clearly defined, however, occurrence of the maximum fluctuating pressure near its center has been established with a fair degree of accuracy.[15,16] The geometry of the vortex street in this intermediate region has its effect on the formation of the turbulent vortex,[11] the Strouhal number,[17] and the mean drag coefficient.[18]

The available information concerning bluff body interaction with the separated flow of stable vortex type is not limited to

Presented as Paper 74-37 at the AIAA 12th Aerospace Sciences Meeting, Washington, D.C., January 30–February 1, 1974; submitted February 19, 1974; revision received October 10, 1974. The investigation reported here was supported by the National Research Council of Canada, Grant Number A-2181.

Index categories: Nonsteady Aerodynamics; Jets, Wakes and Viscid-Inviscid Flow Interactions.

* Professor, Department of Mechanical Engineering. Member AIAA.
† Graduate Research Assistant, Department of Mechanical Engineering.

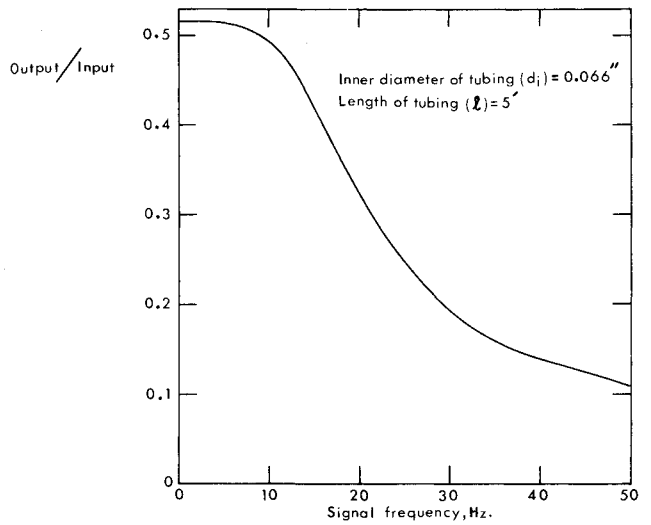

Fig. 1 Calibration plot for Barocel pressure transducer with a damping bottle.

the cylinders of circular cross-section. Investigations with square, rectangular, triangular, and hexagonal cylinders, structural H and angle sections, as well as several irregular geometries, are also reported. But it must be emphasized that the bulk of the literature is indeed devoted to the circular geometry. This point is well emphasized by the fact that the previous work on elliptical cylinders seems to be limited to rather preliminary unsteady pressure measurements by Modi and Heine,[19] Strouhal number study by Schramm,[20] together with fluctuating loading and vortex shedding frequency study by Modi and Wiland.[21]

The significance of elliptic geometry becomes apparent during the study of a circular cylinder in yawed condition. Furthermore, an elliptic section represents a more general configuration permitting realization of a wide range of geometrical shapes, from circular cylinder ($e = 0$) to flat plate ($e = \infty$), by a systematic variation of eccentricity. This is quite useful as it permits one to explore transitional effects of fixed to boundary-layer type separation on the near wake.

This paper studies, experimentally, near wake aerodynamics of two-dimensional elliptic cylinders ($e = 0.44$, 0.80, 0.92, 0.98) during the organized wake condition (Reynolds number = 68,000). In the beginning, results concerning wake geometry and vortex velocity are obtained as functions of cylinder eccentricity and angle of attack. When available, data from the literature (for $e = 0, \infty$) are included for comparison and to help establish trends. This is followed by a detailed scanning of the near wake for unsteady pressure using Barocel Modular Pressure Transducing System (sensitivity, 10^{-6} psi) to provide information about the separating shear layers and formation of the first vortex. Finally, the flowfield is examined visually through the Schlieren technique in conjunction with high-speed photography (1000–2000 frames/sec) to provide, at least qualitatively, some understanding of the complex phenomenon.

II. Test Procedures

Four elliptic cylindrical models, each 27 in. long and having the major axis of 5 in. were designed to span the wind tunnel cross-section, 36 in. × 27 in., thus approximating the two-dimensional flow condition. The models were tested in a low-speed, low-turbulence, return-type wind tunnel where the air speed can be varied from 4–150 fps with a turbulence level less than 0.1%.

Most of the instrumentation used in the experimental program, e.g. wind tunnel balance, manometers, filters, rms meter, etc., constitute standard equipment in any aerodynamics laboratory and hence need no elaboration. The fluctuating pressure measurements were carried out using Barocel Modular Pressure Transducing System developed by Datametrics Inc. of Waltham, Massachusetts. Its constructional details and performance specifications have been described earlier.[21]

The Barocel is accurately calibrated for steady pressures. However, for fluctuating signals transmitted through relatively long, small diameter tubes considerable attenuation would occur. Therefore the output electrical signal required calibration against known input fluctuating pressure at the model surface. This was achieved using the calibration system developed by Modi and Wiland.[21] Figure 1 shows the calibration plot for the transducer in terms of attenuation as a function of signal frequency.

The wake survey was carried out using a disk probe constructed in accordance with the design discussed in detail by Bryer et al.[22] It was mounted on a 1 in. hypodermic needle which, in turn, was connected to a 14 in. long, 1/4 in. diam sting. The mean pressure calibration results for the probe are shown in Fig. 2. The measurements indicate the probe to be relatively insensitive to a pitch of ±5% and yaw of ±20°. The wake traversing gear was used to position the probe at a desired location in the wind tunnel test section. The accuracy in positioning the probe was approximately 0.02 in.

The determination of the wake geometry was accomplished by examining the fluctuating pressure field, associated with the vortices shed from the model, using the instrumentation layout

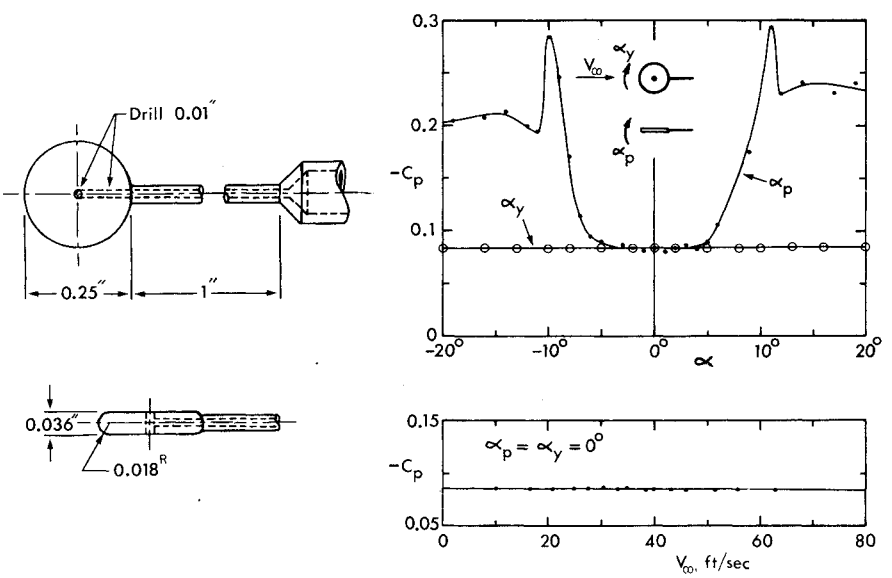

Fig. 2 Disk probe and calibration plots.

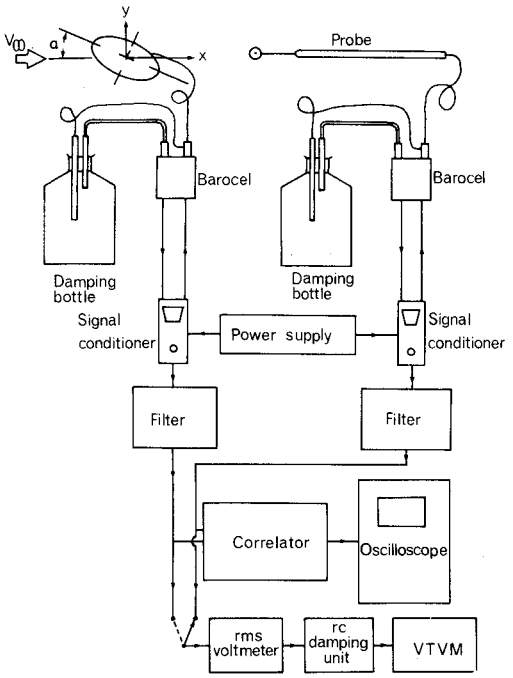

Fig. 3 Schematic diagram of the instrumentation used in the wake survey.

shown in Fig. 3. Traversing the disk probe through the wake at various downstream stations and recording the rms value of the pressure signal gave a set of curves each having two peaks near the vortex center lines. The distance between these maxima, at a given downstream station, was taken to be a measure of the lateral spacing between the two rows of vortices. It was convenient to present the results of each lateral traverse as a ratio of the probe to the model tap rms signals. The selection of the model tap for the ratio was somewhat arbitrary, but represented the position on the model having a near maximum value of the unsteady pressure. The variation of the peak pressure values along the x-coordinate gave an indication as to the position of the first vortex formation and its decay in the downstream direction.

The longitudinal spacing between the consecutive vortices was obtained through recognition of the fact that the distance corresponds to a 360° phase difference between the fluctuating pressure signals associated with them. Using a pressure tap on the model as reference, the disk probe was moved downstream near the center line of a vortex row. The phase data, obtained using a signal correlator, was recorded as a function of the downstream coordinate. The process was continued until limited by the travel of the traversing gear (40 in.). The plot of the phase vs the x-coordinate gave a continuous variation of the longitudinal spacing through the relation

$$L = (dx/d\phi^\circ)(360^\circ) \tag{1}$$

The Strouhal frequency being known, the vortex velocity in the wake was also determined. The wake traverse measurements were confined to the midspan of the models.

In an experimental program of this nature, a question concerning the reliability of the data, which has a philosophical touch to it, naturally arises. More pragmatically, reliability would be governed by the test facility, models, and accuracy of the electronic instrumentation. The relevant details are discussed in Refs. 6, 14, and 21. In general, the results presented can be reproduced within an accuracy of 5%.

III. Results and Discussion

There appears to be rather scant information concerning the organized wake associated with elliptic cylinders. Modi and Wiland[21] presented preliminary results on its near infinity character; i.e., uniform values of vortex spacings attained 5–8 "diam" (major axis) downstream, for cylinders of eccentricity 0.60 and 0.80. However, no attempt was made to explore the variation of wake geometry as a function of the downstream coordinate. This section discusses the results of a detailed investigation on the wake of cylinders with $e = 0.44$, 0.80, 0.92 and 0.98. To study the dependence of various wake parameters on the attitude of the models, the experiments were conducted at $\alpha = 0, 30°, 60°$ and 90°. Since the Reynolds number effect in the range 3×10^4–10^5 is reported to be negligible,[21] all the tests were confined to $R = 68{,}000$. The amount of information obtained through the experimental program is rather enormous, however for conciseness only a few of the typical results sufficient to establish definite trends are included here.

Longitudinal Spacing and Vortex Velocity

The results on phase variation in the downstream direction showed it to attain a constant value suggesting uniform vortex velocity and longitudinal spacing. The limited reach of the traversing gear and poor strength of the fluctuating pressure signal restricted the longitudinal measurements to 8 diam. Fortunately, this does not represent a serious limitation as Frimberger's[23] experiments with circular cylinders in air and water showed the wake geometry to attain uniform dimensions around the same distance downstream. Typical variations of the longitudinal spacing between vortices obtained using Eq. (1) are presented in Fig. 4. The plots show a rapid increase in spacing for the distance of 2–3 diam behind the cylinder, gradually approaching a constant value by 7 diam. In general, a lower angle of attack is accompanied by early attainment of uniform spacing. The vortex spacing showed increase with increase in angle of attack, the larger change, as expected, being associated with high eccentricity ellipses.

The vortex velocity was deduced from the relation,

$$V_v = fL \tag{2}$$

Although V_v shows a trend similar to the longitudinal spacing, it is relatively less dependent on the cylinder attitude and eccentricity. In general the effect of increase in angle of attack and eccentricity is to delay the establishment of near infinity values downstream.

Figure 5 summarizes the dependence of longitudinal spacing at two extreme attitudes of the models. As can be expected, the effect of eccentricity at $\alpha = 90°$ is relatively small. On the other hand, the plots at $\alpha = 0$ show significant dependence on eccentricity. At a given station, the longitudinal spacing increases as the cylinder becomes more slender, which also promotes early attainment of its uniform value. For the ellipses of $e = 0.92$ and 0.44 the near infinity values were reached approximately 3 and 5 diam downstream, respectively. It may be mentioned here that basing downstream distance and longitudinal spacing on minor axis showed reduction in the latter's variation with e at $\alpha = 0$. In particular the near infinity value of the parameter was found to be $\simeq 4$ except for $e = 0.92$ in which case it was 3.2. For other angles of attack the values ranged between 4.0 and 5.5. Of course, a degree of similarity between variation of the dimensionless vortex velocity and longitudinal spacing is expected as the two variables are directly related by the Strouhal number.

Lateral Spacing

Representative plots showing lateral variation of the fluctuating pressure amplitude in the wake at various downstream stations are presented in Fig. 6. Here $\bar{F}$ is a dimensionless pressure parameter representing ratio of the maximum fluctuating pressure (average amplitude based on the rms value) at a transverse station in the wake to the corresponding value on the surface of the model for a given angle of attack.

As expected the unsteady pressure distributions are similar on both sides of the wake for symmetrically oriented models. The wake centerline, thus, coincides with the x-axis. However, for other orientations, the wake is unsymmetrical with the higher

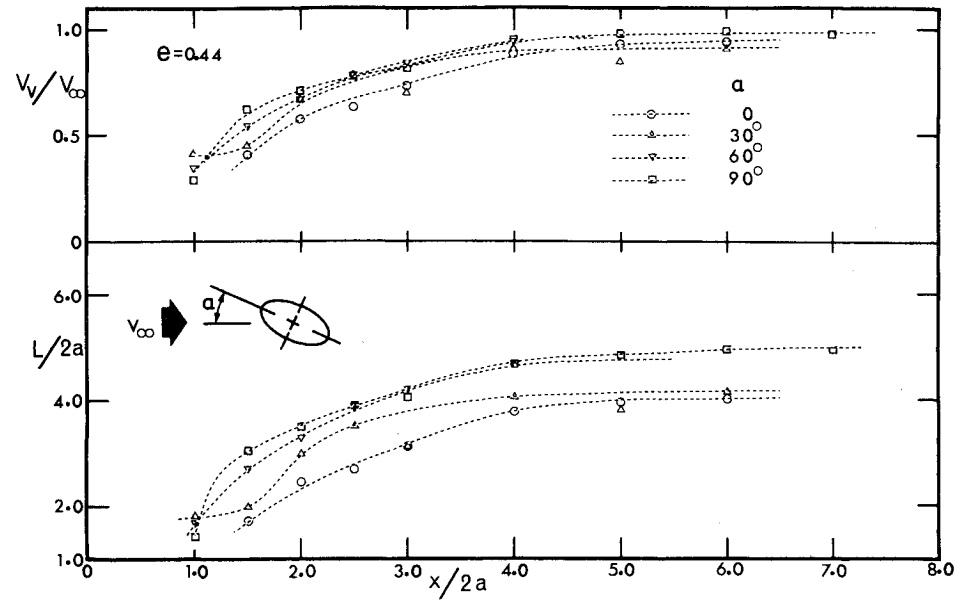

Fig. 4 Streamwise variation of the longitudinal vortex spacing and vortex velocity: a) $e = 0.44$; b) $e = 0.92$.

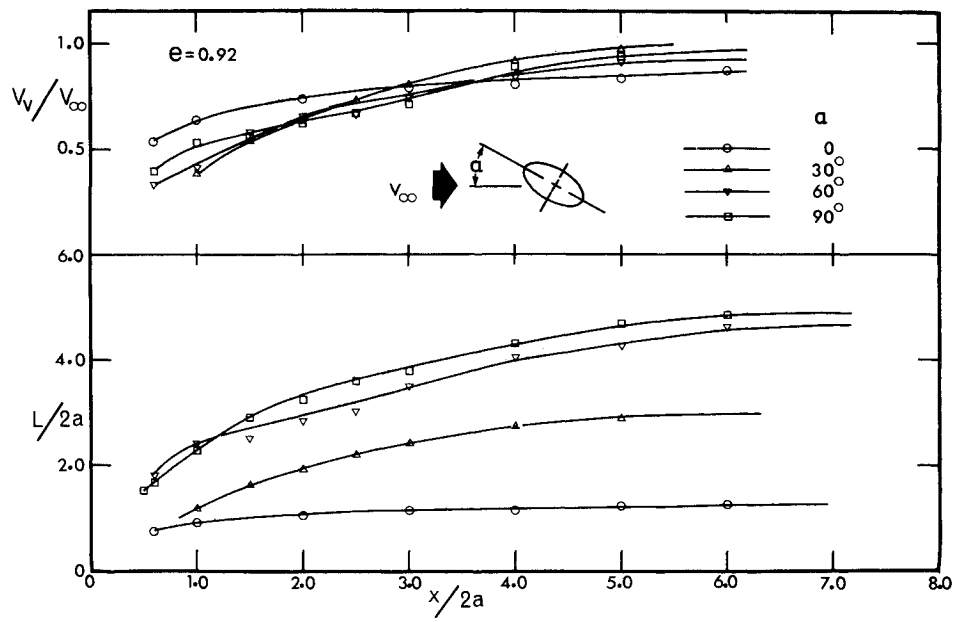

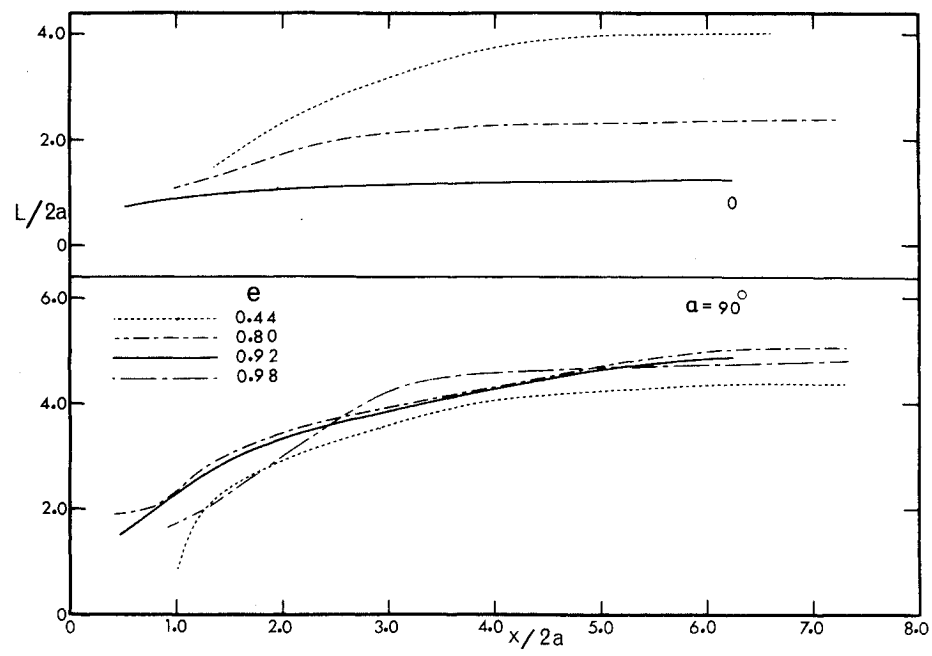

Fig. 5 Dependence of the longitudinal spacing on the cylinder eccentricity at extreme values of the angle of attack.

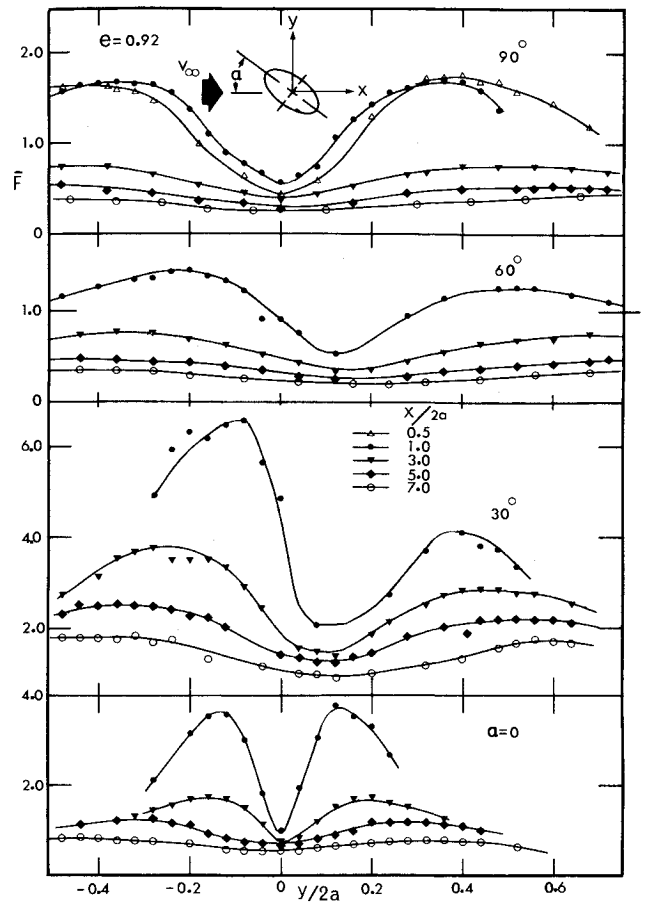

Fig. 6 Lateral variation of the fluctuating pressure in the wake of elliptic cylinders.

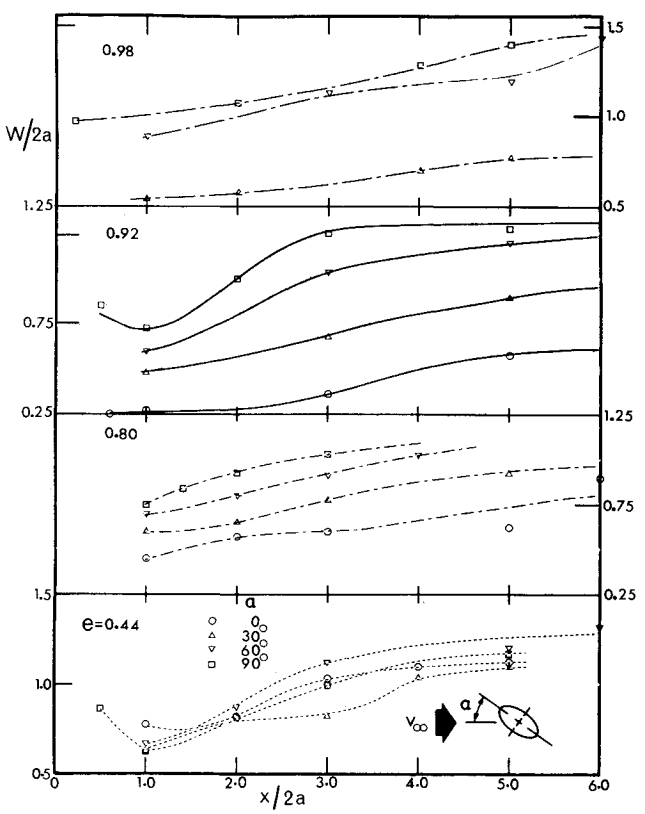

Fig. 7 Variation of the lateral vortex spacing with the downstream coordinate and angle of attack.

Table 1 Variation of the lateral spacing with the downstream coordinate for several bluff bodies

Circular cylinder,[a] $e = 0$, $R = 4{,}900$		Elliptic cylinder $e = 0.92$, $\alpha = 90°$, $R = 68{,}000$		Flat plate[b] $e = \infty$, $\alpha = 90°$, $R = 31{,}000$	
$x/2a$	$W/2a$	$x/2a$	$W/2a$	$x/2a$	$W/2a$
3.22	1.06	1.0	0.72	5.0	1.30
4.60	1.19	3.0	1.20	10.0	2.00
7.00	1.34	5.0	1.20	20.0	2.75
8.80	1.40	7.0	1.40		

[a] Tyler.[27] [b] Fage and Johansen.[24]

peak value on the side for which the separation of the shear layer is more rearward. Similar behavior was also observed by Slater[6] in his study with a structural angle section. As the vorticity rate associated with the upper and lower surfaces of a body is the same,[10] the presence of a higher pressure peak on one side may be explained by relatively shorter distance traveled and hence reduced dissipation suffered by the corresponding vortex. Figure 7 shows the position of the wake obtained by considering, approximately, the location of peak fluctuation as the position of the vortex core. However, as pointed out by Hooker,[16] the maximum velocity fluctuations (and hence pressure variations) do not occur along the path of vortex centers as some experimenters have asserted but rather develop in the neighborhood of the core farthest from the street centerline.

Thus, the distance between the peaks as presented here would overestimate the wake width by an amount equal to the diameter of the vortex core. Based on Schaefer and Eskinazi's[15] mathematical model for the vortex street in viscous fluid showed the correction in the wake width to be negligible ($<1\%$) at the model and less than 5% 8 diam downstream. It may be pointed out, however, that the correction would fail far downstream as it does not account for turbulence or wake instability which would influence the position and growth of the vortex cores.

It is apparent that both the model geometry and attitude have substantial effects on the spacing between the vortex rows. In general, the spacing increased with downstream coordinate except for the short formation region, and in some cases failed to attain the uniform value within the limit of the traverse. As pointed out by several investigators,[24-26] vortices do not flow downstream indefinitely in parallel rows but always move away from the centerline with increasing x even when an intermediate sequence of vortices have some uniformity of configuration. This point is well emphasized by the wake width results for flat plate,[25] circular,[27] and elliptic cylinders presented in Table 1.

Wake Geometry Ratio

Longitudinal and lateral spacing results may be combined to obtain the classical wake geometry parameter, W/L (Fig. 8). With increase in downstream coordinate, in general, there is a drop in the value up to, approximately, 2–4 diam downstream followed by a region of constant value and finally a tendency towards rise in W/L. In particular, for $e = 0.98$, the ratio ranged between 0.4 to 0.6 at $x/2a = 1.0$, diminished to $\simeq 0.3$ in the vicinity of $x/2a = 4.0$, and showed an upward trend thereafter. This corresponds reasonably well with von Kármán's observation of $W/L \simeq 0.36$ behind the body approaching the value 0.281 farther downstream. A rise in the wake geometry ratio when far downstream is also reported by several investigators[24,26] in the flat plate and circular cylinder studies. In fact Fage and Johansen,[24] in their experiment with a flat plate normal to the flow, found W/L to increase by more than 100% over the downstream distance of 5–20 plate widths. It is of interest to note that the location of the minimum wake geometry ratio seems to move downstream with increase in eccentricity of an ellipse. The wake width did not show any well-defined dependence on cylinder attitude.

The near infinity values for the wake width and geometry ratio as affected by cylinder eccentricity and attitude are

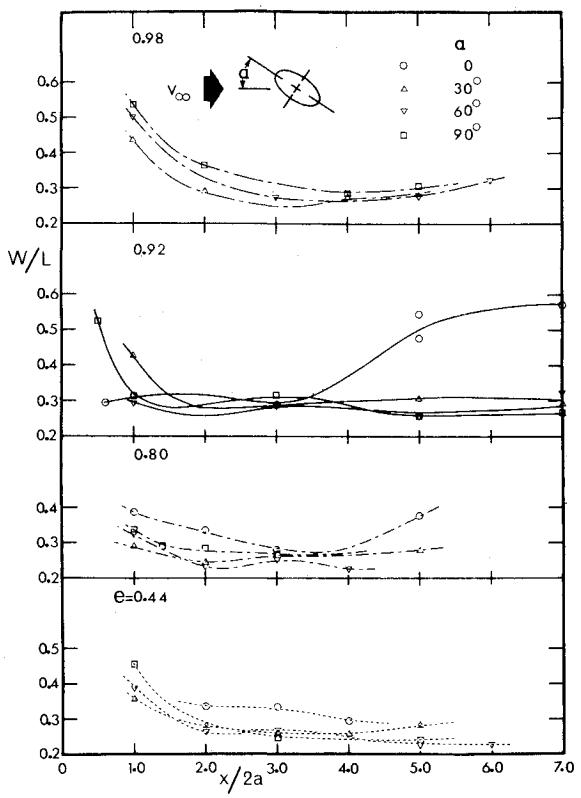

Fig. 8 Wake geometry ratio for elliptic cylinders as a function of the downstream distance.

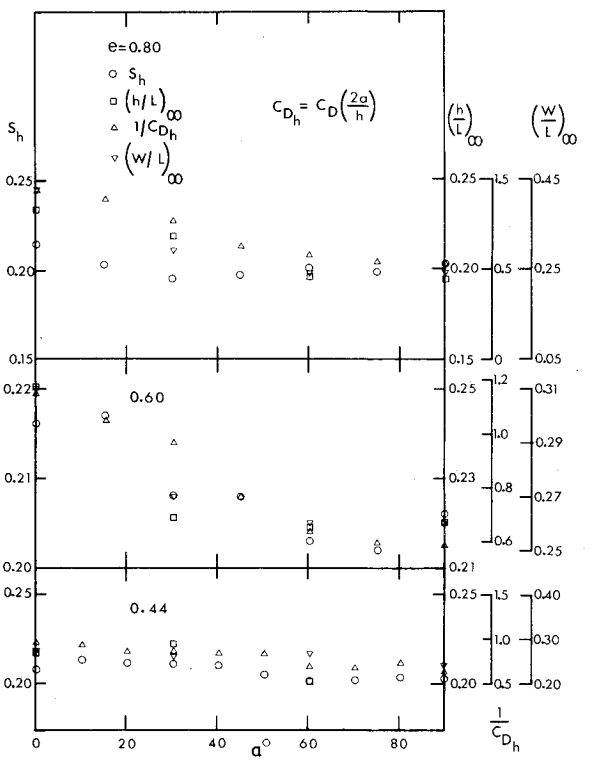

Fig. 9 Variation of the Strouhal number, drag coefficient, and near infinity values of the wake parameters with the cylinder attitude.

summarized in Table 2. The quoted figures occur around 6 to 7 diam downstream. For $\alpha = 0$, the wake width diminishes with increase in eccentricity, however, the wake geometry ratio increases suggesting greater reduction in longitudinal spacing. Essentially the same behavior was observed at $\alpha = 30°$. No clear pattern can be discerned at $\alpha = 60°$; however, at higher attitude, there appears to be a complete reversal in the trend of $(W/2a)_\infty$ observed earlier. Furthermore, the wake geometry ratio remains reasonably close to von Kármán's stability value of 0.281.

It would be appropriate to emphasize a degree of similarity in the variation of $(h/L)_\infty$, $(W/L)_\infty$, S_h and $1/C_{D,h}$ with model orientation. This is shown in Fig. 9. In general they appear to attain the peak value at $\alpha = 0$, diminish with increase in angle of attack to reach a minimum around 50°, followed by a small rise over the remaining range. Apparently this suggests significant relationships between the wake geometry and body aerodynamics. The use of universal numbers in such a study by several authors may be attributed to the similar observation of wake-body interaction. Although not shown here for conciseness, it may be of interest to point out that the use of the projected height as a nondimensionalizing parameter does not significantly reduce variation of the wake parameters with angle of attack.

Vortex Formation Region

The results of lateral traverse also provide information about variation of the peak fluctuating pressure with the downstream coordinate (Fig. 10). It appears that the pressure amplitude attains a maximum value around 1 diam downstream. The pressure decay that follows compares favorably with the analytical results obtained using the vortex street model of Schaefer and Eskinazi.[15] However, a systematic experimental study of its rise and decay in the downstream direction and as a function of the cylinder eccentricity and attitude does not seem to be reported in literature. In general the increase in angle of attack tends to move the pressure peak upstream. This may suggest closer formation of the first vortex at higher angles of attack. The behavior was confirmed through flow visualization.

To obtain some preliminary information concerning the position of the first vortex and hence the vortex formation length[12] as affected by the cylinder eccentricity and angle of attack, a program of high-speed photography (16 mm movie) using the Schlieren technique was undertaken. Several aspects of interest became apparent through the frame-by-frame analysis of the movie: 1) The photographs suggested that the first vortex is located around 0.75–1.5 diam downstream from the cylinder axis.

Table 2 Dependence of the near infinity values for the lateral vortex spacing and wake geometry ratio on the eccentricity and angle of attack

	$\alpha = 0$		$\alpha = 30°$		$\alpha = 60°$		$\alpha = 90°$	
e	$(W/2a)_\infty$	$(W/L)_\infty$	$(W/2a)_\infty$	$(W/L)_\infty$	$(W/2a)_\infty$	$(W/L)_\infty$	$(W/2a)_\infty$	$(W/L)_\infty$
0[a]	1.3–1.8	0.24–0.28						
0.44	1.12	0.27	1.10	0.26	1.28	0.27	1.14	0.23
0.60[b]	1.0	0.31	1.04	0.27	1.14	0.26	1.16	0.25
0.80	0.90	0.38	0.96	0.29	1.12	0.24	1.20	0.24
0.92	0.62	0.48	0.96	0.32	1.25	0.27	1.32	0.27
0.98	...	...	0.78	0.28	1.25	0.28	1.45	0.30
∞[c]	...	...	...	...	...	...	1.65	0.32

[a] Schaefer and Eskinazi.[15] [b] Modi and Wiland.[21] [c] Fage and Johansen.[24]

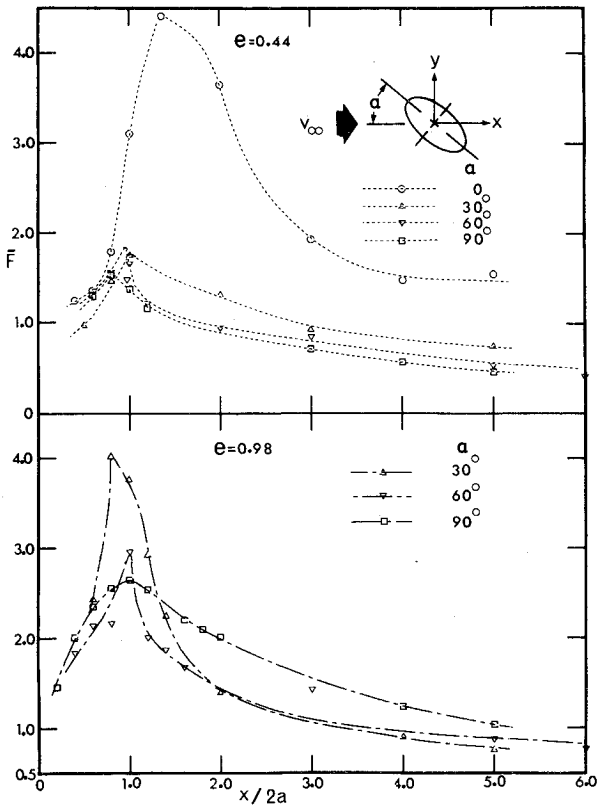

Fig. 10 Variation of peak fluctuating pressure in the wake.

This is in agreement with the location of the fluctuating pressure peaks in Fig. 10. 2) A comparison of vortex positions at $\alpha = 0$ and 90° for a set of ellipses showed forward movement of the first vortex at higher angles of attack. This, in general, confirms the trend indicated by the pressure peaks in the wake. On the other hand, no conclusive remarks can be made about the effect of eccentricity at the same angle of attack. 3) The unsteady character of the position of separation became quite evident. For circular cylinder it was observed to be, approximately, over the range of 70°–88°. This movement is accompanied with the periodic change in inclination of the separating shear layer.

A comment concerning the blockage effects would be appropriate before closing. The blockage ratio during the experimental program varied over the range of 3–14%, corresponding to the ellipse of 0.98 eccentricity at zero angle of attack and models at 90°, respectively. Fortunately, on the basis of an experimental study by Modi and El-Sherbiny[28] with circular cylinders and flat plates of blockage as high as 35.8%, it may be concluded that bluffness effects on wake parameters are likely to be negligible. Hence the results presented here are uncorrected for blockage.

IV. Conclusions

Based on the present experimental results and other reported investigations, the following general remarks can be made concerning aerodynamics of the near wake associated with stationary elliptic cylinders.

1) It is of interest to recognize, on the basis of results reported in the literature, that both longitudinal and lateral spacings between the vortices are substantially independent of the Reynolds number in the subcritical range. Longitudinal spacing between vortices increases rapidly behind the model and attains a constant value around 7 diam (limit of the traversing gear) downstream. It increases with increase in angle of attack, the larger change being associated with high eccentricity ellipses. The vortex velocity has relatively small dependence on attitude and eccentricity of an ellipse. The lateral spacing continues to increase with the downstream coordinate, for some cases even beyond the limit of the traverse. At small angles of attack, the effect of increase in eccentricity is to diminish the wake width. However, at $\alpha = 90°$, the trend undergoes a complete reversal. A certain amount of similarity can be discerned between the variation of $(h/L)_\infty$, $(W/L)_\infty$, S_h and $1/C_{D,h}$ with angle of attack. This emphasizes the interaction between wake geometry and body aerodynamics. In general, the wake geometry ratio remains close to the von Kármán stability value of 0.281.

2) The rise and decay of fluctuating pressure in the wake suggests the formation of the first vortex to occur in the vicinity of 1 diam downstream. The flow visualization confirms this observation.

3) The high-speed Schlieren photography indicates, qualitatively, unsteady character of the position and inclination of the separating shear layers.

References

[1] Rosenhead, L., "Vortex Systems in Wakes," *Advances in Applied Mechanics*, Vol. 3, Academic Press, New York, 1953, pp. 185–195.

[2] Wille, R., "Über Stromungserscheinungen im Übergangsgebiet von geordneter zu ungeordneter Bewegung," *Jahrbuch der Schiffbautechnik Gesellschaft*, Vol. 46, 1952, pp. 176–187.

[3] Wille, R., "Kármán Vortex Streets," *Advances in Applied Mechanics*, Vol. 6, 1960, pp. 273–287.

[4] Marris, A. W., "A Review on Vortex Streets, Periodic Wakes, and Induced Vibration Phenomena," *Transactions of the ASME, Journal of Basic Engineering*, Ser. D, Vol. 86, 1964, pp. 185–196.

[5] Morkovin, M. V., "Flow Around Circular Cylinder—A Kaleidoscope of Challenging Fluid Phenomena," *ASME Symposium on Fully Separated Flows*, 1964, pp. 102–118.

[6] Slater, J. E., "Aeroelastic Instability of a Structural Angle Section," Ph.D. thesis, March 1969, Department of Mechanical Engineering, University of British Columbia, Vancouver, B.C., Canada.

[7] Hinze, J. O., *Turbulence*, McGraw-Hill, New York, N.Y., 1959, Ch. 6.

[8] Bloor, M. S. and Gerrard, J. H., "Measurements on Turbulent Vortices in a Cylinder Wake," *Proceedings of the Royal Society of London*, Ser. A, Vol. 294, 1966, pp. 319–342.

[9] Bloor, M. S., "The Transition to Turbulence in the Wake of a Circular Cylinder," *Journal of Fluid Mechanics*, Vol. 19, 1964, pp. 290–304.

[10] Fage, A. and Johansen, F. C., "The Structure of Vortex Sheets," *The Philosophical Magazine*, Ser. 7, Vol. 5, No. 28, 1928, pp. 417–441.

[11] Abernathy, F. H. and Kronauer, R. E., "The Formation of Vortex Streets," *Journal of Fluid Mechanics*, Vol. 13, 1961, pp. 1–20.

[12] Gerrard, J. H., "The Mechanics of the Formation Region of Vortices Behind Bluff Bodies," *Journal of Fluid Mechanics*, Vol. 25, Pt. 2, 1968, pp. 401–413.

[13] Roshko, A., "On the Drag and Shedding Frequency of Two-Dimensional Bluff Bodies," TN-3169, 1953, NACA.

[14] Dikshit, A. K., "On the Unsteady Aerodynamics of Stationary Elliptic Cylinders During Organised Wake Condition," M.A.Sc. thesis, July 1970, Department of Mechanical Engineering, Univ. of British Columbia, Vancouver, B.C., Canada.

[15] Schaefer, J. W. and Eskinazi, S., "An Analysis of the Vortex Street Generated in a Viscous Fluid," *Journal of Fluid Mechanics*, Vol. 6, 1959, pp. 241–260.

[16] Hooker, S. G., "On the Action of Viscosity in Increasing the Spacing Ratio of a Vortex Street," *Proceedings of the Royal Society of London*, Ser. A, Vol. 154, 1936, pp. 67–89.

[17] Bearman, P. W., "On Vortex Street Wakes," *Journal of Fluid Mechanics*, Vol. 28, 1967, pp. 625–641.

[18] von Kármán, Th., "Flüggigkeit u. Luftwiderstand," *Zeitschrift fuer Physik*, Vol. 13, 1911, p. 49; "Über den Mechanismus des Flüssigkeits -und Luftwiderstandes," *Zeitschrift fuer Physik*, Vol. 13, 1912, pp. 49–59; "Über den Mechanismus des Widerstands, den ein bewegter Körper in einer Flüssigkeit erfährt," *Gottinger Nachrichten*, Mathematische Physik, K1, 1911, pp. 509–519; 1912, pp. 547–556.

[19] Modi, V. J. and Heine, W., "On the Pressure Fluctuations and Wake Geomentry Associate with Several Bluff Bodies," *JSME Proceedings of the 15th Japan National Congress of Applied Mechanics*, 1965, pp. 7–18.

[20] Schramm, W., "Wirbelfrequenzmessungen an umströmten Bauteilen," Institut für Leichtbau–Mitteilungen, Vol. 5, No. 8, 1966, pp. 308–318.

[21] Modi, V. J. and Wiland, E., "Unsteady Aerodynamics of Stationary Elliptic Cylinders in Subcritical Flow," *AIAA Journal*, Vol. 8, Oct. 1970, pp. 1814–1821.

[22] Bryer, D. W., Walshe, D. E., and Garner, H. C., "Pressure Probes Selected for Three-Dimensional Flow Measurement," R. and M. No. 3037, 1958, Aeronautical Research Council, London.

[23] Frimberger, R., "Experimentelle Untersuchungen an Kármánschen Wirbelstrassen," *Zeitschrift Flugwiss*, Vol. 5, 1957, pp. 355–359.

[24] Fage, A. and Johansen, F. C., "On the Flow of Air Behind an Inclined Flat Plate of Infinite Span," *Proceedings of the Royal Society of London*, Ser. A, Vol. 116, 1927, pp. 170–197.

[25] Rosenhead, L. and Schwabe, M., "An Experimental Investigation of the Flow Behind Circular Cylinders in Channels of Different Breadths," *Proceedings of the Royal Society of London*, Ser. A, Vol. 129, 1930, pp. 115–135.

[26] Wille, R. and Timme, A., "Über des Verhalten von Wirbelstrassen," *Jahrbuch der Schiffbautechnik Gesellschaft*, Vol. 51, 1957, pp. 215–221.

[27] Tyler, E., "Vortex Formation Behind Obstacles of Various Sections," *The Philosophical Magazine*, Ser. 7, Vol 11, No. 72, 1931, pp. 849–890.

[28] Modi, V. J. and El-Sherbiny, S., "On the Wall Confinement Effects in the Industrial Aerodynamics," Paper 116, *Proceedings of the International Symposium on Vibration Problems in Industry*, U.K. Atomic Energy Authority and National Physical Lab., Keswick, England, 1973.

APRIL 1975 AIAA JOURNAL VOL. 13, NO. 4

Unsteady Aerodynamics of Vehicles in Tubes

ANDREW G. HAMMITT*
Andrew G. Hammitt Associates, Palos Verdes Peninsula, Calif.

The aerodynamics of vehicles traveling through tubes are significantly affected by the constraints of the tube wall and the relative size (blockage ratio) of the vehicle. Steady flow conditions are reached only after long travel times. In this report, the flow created by vehicle travel in a tube is analyzed using numerical integration of the unsteady flow equations. Steady state conditions are rarely obtained for closed-end tubes up to several hundred miles in length. Solutions are presented for various blockage ratio vehicles with choked and unchoked flow conditions about them. Various tube lengths are also considered. The solution for a doubly infinite tube is found to be approaching the asymptotic long time solution.

Nomenclature

A = cross section area of tube
A_{vw} = vehicle surface area
A_{ww} = tube surface area
C_D = drag coefficient of vehicle based on tube area and relative velocity
C_F = skin-friction coefficient
C_p = specific heat, at constant pressure
C = speed of sound
C_{MT} = momentum loss coefficient of vehicle based on tube area and relative velocity
C_H = Stanton number
d = tube diameter
D = drag of vehicle
L = length of vehicle
m = mass flux
M_∞ = $u_s/(\gamma RT_w)^{1/2}$ vehicle Mach number
p = pressure
p^* = p/p_∞
q_r = heat flux to vehicle
q_w = heat flux to wall
R = gas constant
Re_d = Reynolds number based on tube diameter and vehicle velocity
s = entropy
t = time
T = temperature
T^* = T/T_w
T_o = stagnation temperature of air
T_w = temperature of wall
T_{ow} = stagnation temperature of wall
T_{aw} = adiabatic wall temperature
u = velocity of air relative to tube
u^* = u/u_s
u_s = velocity of vehicle relative to tube
v = velocity of air relative to vehicle, $v = u - u_s$
v^* = v/u_s
x = distance along tube
β = vehicle area blockage ratio, area of vehicle/area of tube
γ = specific heat ratio
λ = $2C_f L/(1-\beta)$
ρ = fluid density
τ_w = wall shear stress
τ_v = vehicle surface shear stress

Received March 7, 1974; revision received October 15, 1974. This work was sponsored by Office of Research, Development and Demonstrations, Federal Railroad Administration, U.S. Department of Transportation.

Index categories: Nonsteady Aerodynamics; Nozzle and Channel Flow.

* President. Member AIAA.

Introduction

THE interest in high-speed ground transportation has lead to a variety of suggested systems. Because the aerodynamic drag of a ground vehicle when operating at high speed in the open is quite large, it has been suggested that vehicles be placed in evacuated or semi-evacuated tubes. A necessary step in the development of such systems is an understanding of the applicable aerodynamics. The presence of the tube has two important effects: 1) it restricts the free passage of air about the vehicle, and 2) it confines the disturbances which originate at the vehicle from dissipating in three dimensions. Tube vehicle systems can be classified in many ways. For aerodynamic purposes, the most important parameters are the speed and blockage ratio of the vehicle, the tube length, and the means of propulsion. The importance of speed and blockage are obvious. If the tube is sufficiently long or the time of travel of the vehicle is sufficiently short, then the vehicle behavior will not be influenced by the tube ends. The type of propulsion system which is used has an important influence on the system design and